

Designing Circle Swimmers: Principles and Strategies

Zhiyu Cao,¹ Huijun Jiang,¹ and Zhonghuai Hou^{1, a)}

Department of Chemical Physics & Hefei National Laboratory for Physical Sciences at Microscales, iChEM, University of Science and Technology of China, Hefei, Anhui 230026, China

(Dated: 22 December 2021)

Various microswimmers move along circles rather than straight lines due to their swimming mechanisms, body shapes or hydrodynamic effects. Here, we adopt the concepts of stochastic thermodynamics to analyze circle swimmers confined in a two-dimensional plane, and study the trade-off relations between various physical quantities such as precision, energy cost and rotational speed. Based on these findings, we predict principles and strategies for designing microswimmers of special optimized functions under limited energy resource conditions, which will bring new experimental inspiration for designing smart motors.

PACS numbers: 05.40.-a, 05.70.Ln, 02.50.Ey

I. INTRODUCTION

Microswimmers are intrinsically far away from equilibrium by continuously transferring internal or external energy into their mechanical motion¹⁻⁵. From biological motors, bacteria to synthetic active colloids, a large amount of microswimmers have received great attentions due to their nontrivial dynamical behaviors forbidden in equilibrium systems⁶⁻¹¹. Due to their self-propulsion motions, microswimmers serve as good candidates for cargo-carriers in the realm of natural or man-made micro-machines, which are of significant interest for applications such as drug delivery, biosensing, or shuttle-transport of living cells and emulsion droplets¹²⁻¹⁶, to list a few.

In particular, circle swimmers moving in curved trajectories have been widely applied in cargo delivery¹⁷⁻²⁷. For instance, the sperm-flagella driven Micro-Bio-Robot (MBR) has been reported to perform precisely point-to-point closed-loop motion under the influence of external magnetic field with applications towards targeted drug delivery and microactuation²⁸⁻³⁰. Synthetic catalytic bimetallic nanomotors have been engineered to pick up, haul, and release micrometer-scale cargo with constant velocity circular movements to mimic nanoscale biomotors in biological systems³¹⁻³³. Magnetic swimmers actuated by externally applied field, rotating at a constant speed in a plane, have been envisaged for targeted drug delivery³⁴, and so on. Since such microswimmers generally function at small scales, their transport dynamics are intrinsically stochastic. Therefore, how to work against such inherent fluctuations with good performance is of great importance for their designs^{24,35-37,52,53}.

Here, we address such an issue by studying a general model of Brownian circle swimmer in a 2D plane (see Fig.1), subjected to an active force with constant amplitude F_0 , an internal torque M and an external harmonic potential with strength k . By using the framework of

stochastic thermodynamics⁴⁰⁻⁴³, we have analyzed the heat dissipation of the system as a function of F_0 , M and k , identified as thermodynamic cost of the swimmer. Interestingly, we find that there exists an optimal torque such that the cyclic cost Q_{cyc} could reach a minimum value, which serves as a lower bound for the cost to sustain a stable circular motion. In addition, a trade-off relation between the precision of the circular motion and the thermodynamic cost has been found, indicating that an increased energy supply is needed to maintain punctual transport process as expected. By utilizing the thermodynamic uncertainty relations (TURs)⁴⁴, we have also obtained an analytical expression for the transport efficiency χ_θ , which properly quantifies the performance of the swimmer to work with large speed, high precision, but low cost. With these results, we are able to propose proper strategies for designing swimmers under certain constraints, for instance, when the cyclic energy supply Q_0 is limited. Analysis shows that the maximum χ_θ increases with increasing Q_0 , which can be further enhanced by increasing the external potential strength k . Finally, we illustrate our predicted design principles and strategies by numerical simulations.

II. MODEL

As shown in Fig.1, we consider a microswimmer performing circular motion, carrying cargo along a fluctuating circular orbit in two-dimensional xy plane from A (the start point) to B (the destination) and then going back, which completes a single cyclic transport task. These microswimmers can be natural or synthetic, such as bacteria, rods, or spherical Janus particles, *etc*³⁶, and related scenarios have been reported in environmental remediation, targeted drug delivery or transportation of cells¹⁴.

For simplicity, we model the circle swimmer by an active spherical particle of radius R . The particle is subjected to a self-propelled force with amplitude F_0 along the orientation $\mathbf{e} = (\cos \varphi, \sin \varphi)$ and an internal torque Ω (along the z direction) that drives the circular mo-

^{a)}E-mail: hzhlj@ustc.edu.cn

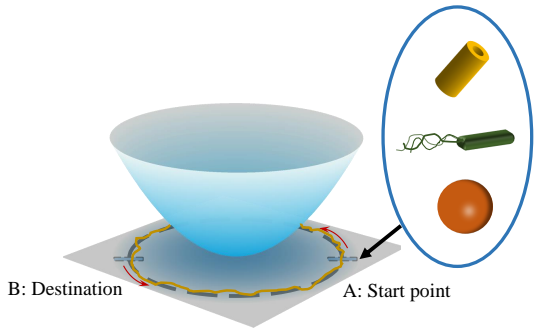


FIG. 1. Schematic sketch of cargo delivering by various types of Brownian circle swimmers. The circle swimmers deliver the cargo from A (start point) to B (destination) along a fluctuating circular orbit (the black line). One may control the swimmer motion by changing its active torque for circular motion, active force for translational motion or by applying possible external potentials (blue surface). The yellow curved line represents the actual stochastic trajectory, and the black dashed line represents the averaged trajectory.

tion. Without loss of generality, we also consider that the particle is controlled by an external conservative force $\mathbf{F}_k(\mathbf{r}) = -\partial_{\mathbf{r}}U_k(\mathbf{r})$ with $U_k(\mathbf{r})$ the external potential (k is a control parameter) and $\mathbf{r} = (x, y)$ the center-of-mass position of the particle. Neglecting hydrodynamic effects, the particle dynamics can be described by the following overdamped Langevin equations:

$$\gamma_t \dot{\mathbf{r}} = \mathbf{F}_k + F_0 \mathbf{e} + \boldsymbol{\xi}, \quad (1)$$

$$\dot{\varphi} = \Omega + \zeta, \quad (2)$$

where γ_t is the translational friction coefficient. For simplicity, we have set the rotational friction coefficient $\gamma_r = 1$ throughout the paper, thus the angular velocity of swimmer equals to the value of torque Ω . The fluctuation terms, $\boldsymbol{\xi} = \{\xi_x, \xi_y\}$ and ζ , are both independent Gaussian white noises with zero mean, satisfying $\langle \boldsymbol{\xi}(t)\boldsymbol{\xi}(s) \rangle = 2\mathbf{I}\gamma_t T\delta(t-s)$ and $\langle \zeta(t)\zeta(s) \rangle = 2T\delta(t-s)$, where T is the ambient temperature and \mathbf{I} the unit tensor. According to (the fluctuation-dissipation relation), the short-time translational and rotational diffusion coefficients of the particle read $D_t = T/\gamma_t$ and $D_r = T$ (where we have set Boltzmann constant $k_B = 1$), with $D_t/D_r = 4R^2/3$ holding for a spherical particle²⁴. The corresponding Fokker-Planck equation for the probability density function $P(\mathbf{r}, \varphi; t)$ is given by

$$\partial_t P(\mathbf{r}, \varphi; t) = -\partial_{\mathbf{r}} \cdot \mathbf{J}_{\mathbf{r}}(\mathbf{r}, \varphi; t) - \partial_{\varphi} J_{\varphi}(\mathbf{r}, \varphi; t), \quad (3)$$

where the probability currents read

$$\mathbf{J}_{\mathbf{r}}(\mathbf{r}, \varphi; t) = \gamma_t^{-1} (\mathbf{F} + F_0 \mathbf{e} - T\partial_{\mathbf{r}}) P(\mathbf{r}, \varphi; t)$$

and

$$J_{\varphi}(\mathbf{r}, \varphi; t) = (\Omega - T\partial_{\varphi}) P(\mathbf{r}, \varphi; t)$$

respectively. Hereafter, we mainly focus upon the steady state with $\partial_t P_{ss}(\mathbf{r}, \varphi) = 0$.

To deliver cargo with good performance for the swimmer considered here, it may be required that the swimmer can reach the destination with a high speed and precisely on time, but with relatively low dissipation⁴⁵. Therefore, fast delivery with high accuracy and low cost can be viewed as a design principle of the swimmer.

III. THERMODYNAMIC COST

To establish a quantitative measure of such a principle, firstly, one needs to investigate the cost of the delivery process. Since the swimmer follows stochastic dynamics, here we use the strategy of stochastic thermodynamics⁴⁰, which has been widely studied in the last decade. Note that the stochastic thermodynamic has been successfully generalized to active matter systems^{46–57}. For instance, Pearce and Giomi have studied the linear response to leadership, effective temperature and decision making for a collection of flocking agents⁴⁷. Kyriakopoulos *et.al* have investigated the nonequilibrium response of polar ordered active fluid to external alignments⁴⁸. Besides, Burkholder and Brady have obtained a generalized fluctuation-dissipation relationship for active suspensions with time-reversal symmetry broken⁵⁵. More recently, Szamal have proposed a generalization of the standard stochastic thermodynamics to self-propelled particles⁵⁷.

The framework of stochastic thermodynamics allows us to calculate the average entropy production and then heat dissipation rate Σ along a delivery cycle, which can be identified as the thermodynamic cost for the delivery process. Following Seifert's spirit⁴⁰, one can define a trajectory-based entropy for the the microswimmer as $s(t) = -\ln P(\mathbf{r}, \varphi; t)$, the change rate of which can be written as

$$\dot{s}(t) = \dot{s}_{tot}(t) - \dot{s}_m(t) \quad (4)$$

where

$$\dot{s}_m(t) = [(\mathbf{F} + F_0 \mathbf{e}) \cdot \dot{\mathbf{r}} + \Omega \dot{\varphi}] / T \quad (5)$$

is the so called medium entropy production⁵⁷ that can be related directly to the heat dissipation rate \dot{q} via $\dot{q} = T\dot{s}_m(t)$. The term $\dot{s}_{tot}(t) = \dot{s}(t) + \dot{s}_m(t) = -\partial_t \ln P(\mathbf{r}, \varphi; t) + T^{-1}\gamma_t \mathbf{v}_r(\mathbf{r}, \varphi; t) \cdot \dot{\mathbf{r}} + T^{-1}v_{\varphi}(\mathbf{r}, \varphi; t) \dot{\varphi}$ is the change rate of the trajectory-dependent total entropy production, where $\mathbf{v}_r = \mathbf{J}_r/P$ and $v_{\varphi} = J_{\varphi}/P$ are the local mean velocities⁴⁰. Upon averaging over trajectories, one can obtain

$$\begin{aligned} \dot{S}_{tot} &= \langle \dot{s}_{tot} \rangle \\ &= T^{-1} \int d\mathbf{r} d\varphi (\gamma_t \mathbf{v}_r^2 + v_{\varphi}^2) P(\mathbf{r}, \varphi; t) \geq 0. \end{aligned} \quad (6)$$

In the steady state, we can use $\Sigma = T \langle \dot{s}_m \rangle = T \dot{S}_{tot}$ to calculate the heat dissipation rate, i.e., the rate of thermodynamic cost for the delivery process. To be specific,

we now set the external potential $U(\mathbf{r}) = k\mathbf{r}^2/2$, where the potential strength k works as a control parameter. For further purpose, it is convenient to rewrite Eq.1 in polar coordinates ($\mathbf{r} = r e^{i\theta}$):

$$\dot{r} = -\beta D_t k r + \beta D_t F_0 \cos(\theta - \varphi) + \sqrt{2D_t} \xi_r, \quad (7)$$

$$\dot{\theta} = -\frac{\beta D_t F_0}{r} \sin(\theta - \varphi) + \sqrt{2D_t} \xi_\theta, \quad (8)$$

where $\xi_r = \cos\theta \xi_x + \sin\theta \xi_y$, $\xi_\theta = -(\sin\theta \xi_x - \cos\theta \xi_y)/r$. In the steady state, the angles θ and φ would be phase-locked, i.e., $\theta - \varphi \simeq \text{const}$ and $\langle \dot{\theta} \rangle \simeq \Omega$. The circle swimmer will rotate along a stochastic limit cycle, and the mean radius of the circular orbit can be computed by setting $\beta D_t k r_m \simeq \beta D_t F_0 \cos(\theta - \varphi)^{24}$, i.e.,

$$r_m = \frac{F_0}{\sqrt{\gamma_t^2 \Omega^2 + k^2}}, \quad (9)$$

where we have used $-\beta D_t F_0 \sin(\theta - \varphi)/r_m \simeq \Omega$. Using Eq.6, one can then obtain the cost rate in the steady state as (see Appendix A for details)

$$\begin{aligned} \Sigma &\simeq \gamma_t \omega^2 r_m^2 + \omega^2 \\ &= \frac{F_0^2 \Omega^2}{\gamma_t \Omega^2 + \gamma_t^{-1} k^2} + \Omega^2. \end{aligned} \quad (10)$$

IV. OPTIMAL TORQUE FOR CYCLIC COST

From Eq.10, one can see that the cost rate depends on all the parameters, the active force F_0 , the torque Ω , the external force strength k , as well as the friction coefficients γ_t . In general, larger activity and torque will lead to larger cost rate, while stronger control (larger k) will reduce the cost rate. Nevertheless, due to the circular motion of the swimmer, a more relevant quantity in real processes would be the cyclic cost Q_{cyc} , i.e., the thermodynamic cost per delivery cycle, which is given by

$$\begin{aligned} Q_{cyc} &= \left(\frac{2\pi}{\Omega}\right) \Sigma \\ &= \frac{2\pi}{\Omega} \left(\frac{F_0^2 \Omega^2}{\gamma_t \Omega^2 + \gamma_t^{-1} k^2} + \Omega^2 \right). \end{aligned} \quad (11)$$

It can be seen that, while smaller torque Ω leads to smaller cost rate Σ , it also causes longer cyclic process. An interesting result is then there exists a trade-off between speed and thermodynamic cost for the circular motion. In particular, an optimal torque Ω_{opt} exists for the circle swimmer to minimize the cost per cycle, which can be obtained by setting $dQ_{cyc}/dM = 0$, giving

$$\Omega_{opt}^2 = \frac{-(\gamma_t^{-1} F_0^2 + 2\gamma_t^{-2} k^2) + \sqrt{\gamma_t^{-2} F_0^4 + 8F_0^2 k^2 \gamma_t^{-3}}}{2}. \quad (12)$$

Note that the condition for the existence of the optimal torque is that the active and external forces must satisfy $k \leq k_0 = \sqrt{\gamma_t F_0^2}$, and the minimum Q_{cyc}^{opt} provides a lower bound of the energy to sustain the circular motion. In the simple case when the external potential is absent ($k = 0$), the optimal torque reads $\Omega_{opt} = F_0/\sqrt{\gamma_t}$, and the corresponding minimum cyclic cost reads $Q_{cyc}^{opt} = 4\pi F_0/\sqrt{\gamma_t}$. With increasing k , it can be observed from Eq.11 that the minimum cyclic cost can be further reduced. If lowering Q_{cyc} is the target for the delivery process, Eqs.(11) and (12) serve as the formula for design principles.

V. PRECISION-COST TRADE-OFF RELATION

Besides thermodynamic cost, another important aspect of the cyclic delivery process is the precision. Similar to biochemical oscillation processes, the precision can be conveniently measured by the phase diffusion constant $D_\theta = (\langle \theta^2 \rangle - \langle \theta \rangle^2)/2t$. Using similar method as in our previous work⁵⁸, we can obtain

$$D_\theta \simeq \frac{D_t}{r_m^2} = \frac{T(\gamma_t \Omega^2 + \gamma_t^{-1} k^2)}{F_0^2}. \quad (13)$$

Combining this result with Eq.(10), we reach an interesting trade-off relation between phase diffusion and dissipation rate, which reads,

$$D_\theta = \frac{T\Sigma_c}{\Sigma - \Sigma_c}, \quad (14)$$

where $\Sigma_c = \Omega^2$ can be identified as the minimum dissipation rate of a circular motion.

A few remarks can be made. Firstly, large dissipation rate is required to reach high precision, which exactly tells the trade-off between cost and gain. Secondly, for a circle swimmer carrying cargo, the dissipation rate needs to exceed a critical value Σ_c to transport along the rotational orbit, which is already indicated in Eq.(10), and extra dissipation could be applied to ensure the swimmer works with a more punctual manner. Thirdly, the inverse law, Eq.14, between phase diffusion constant D_θ and dissipation rate Σ has also been found in biochemical oscillation systems^{58,59}, highlighting its ubiquitous importance in living systems.

VI. TRANSPORT EFFICIENCY

To further characterize the performance and design principle of the circle swimmer, here we apply the so-called thermodynamic uncertainty relation (TUR), which was first proposed by Barato and Seifert⁴⁴ in Markovian jump processes, and has been extensively studied recently⁶⁰⁻⁶⁷. According to Dechant and Sasa⁶⁸, a TUR relation holds for general Langevin systems as

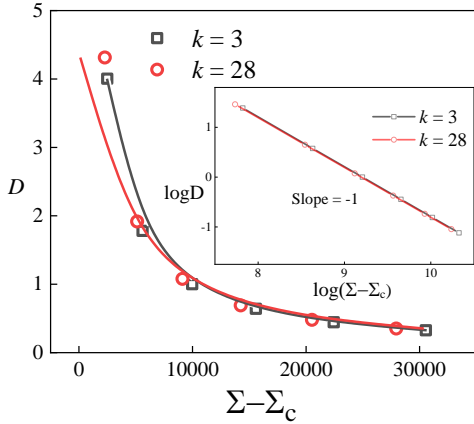


FIG. 2. (a) The trade-off relation Eq.14 between the normalized phase diffusion constant $D = D_\theta/T$ and the dissipation rate Σ . The symbols are obtained from numerical results and solid curves are the theoretical expressions. The data plotted in log-log scale are fitted well by the scaling form $D = \Sigma_c (\Sigma - \Sigma_c)^\alpha$ with fitting parameter $\alpha = -1$ (inset).

$(v_j^{st})^2 / \dot{S}_{tot} D_j \leq 1$, wherein v_j^{st} and D_j are steady state velocity and diffusivity of a generalized current variable j , respectively. Note that such a relation implies that one cannot obtain an arbitrary large speed without either accepting large phase diffusion or investing a large dissipation, which exactly tells the trade-off among speed, precision and energy cost. Direct application of the TUR to our present system, choosing j as θ , is that

$$\chi_\theta = (v_\theta^{st})^2 / \dot{S}_{tot} D_\theta \leq 1$$

where χ_θ is the transport efficiency^{45,68}. Clearly, χ_θ can be used to quantitatively describe the ability for the swimmer to maintain a high-speed, accurate transport with lower dissipation. Combining Eq.10 and 13, noting that $v_\theta^{st} = \Omega$, we obtain the theoretical expression of the transport efficiency for the circle swimmer as

$$\chi_\theta = \frac{F_0^2}{F_0^2 + \gamma_t \Omega^2 + \gamma_t^{-1} k^2}. \quad (15)$$

which is clearly less than 1 for nonzero Ω or k . Obviously, a larger self-propelled force will increase the transport efficiency, while a larger torque or potential strength will reduce it.

VII. DESIGN STRATEGY FOR LIMITED ENERGY RESOURCE

For better performance of the swimmer regarding cargo delivery, it is suggested that χ_θ should be as large as possible. To this goal, it seems that one can simply enhance the activity (F_0) and reduce the torque (Ω) or external potential (k). However, as discussed above, increasing F_0

will also increase the thermodynamic cost rate Σ or the cyclic cost Q_{cyc} . In real systems, a more relevant question would be how to design the circle swimmer when the energy resource is limited. For instance, when the chemical substances driving the directional movement are exhausted, the microswimmers may fail to self-propelled³¹. Here, we focus on a situation when the cyclic supply of energy is limited by a given value Q_0 , and discuss how to maximize the transport efficiency χ_θ under such a constraint. Note that to sustain the rotation motion, Q_0 must be larger than the minimum value Q_{cyc}^{opt} given by Eq.(11). If not, a feasible way is to increase the external potential strength k and thus reduce Q_{cyc}^{opt} as indicated also in Eq.(11). A simple analysis shows that setting the strength $k \geq \sqrt{\gamma_t \left(\frac{2\pi F_0^2 \Omega}{Q_0 - 2\pi \Omega} - \gamma_t \Omega^2 \right)}$ can make the swimmer maintain circular motion in the case when $Q_0 < 4\pi F_0 / \sqrt{\gamma_t}$.

Given that $Q_0 > 4\pi F_0 / \sqrt{\gamma_t}$, circular motion can be sustained in the absence of external potential, i.e., $k = 0$. For now, the design principle is to maximize the transport efficiency $\chi_\theta = F_0^2 / (F_0^2 + \gamma_t \Omega^2)$ under the constraint that $Q_{cyc}(F_0, \Omega) = 2\pi \left(\frac{F_0^2}{\gamma_t \Omega} + \Omega \right) \leq Q_0$. The conditional highest transport efficiency, which is achieved when $Q_{cyc} = Q_0$, can be obtained as (see Appendix B for details)

$$\chi_{\theta, \max} = \left[1 + \frac{4}{(C + \sqrt{C^2 - 4})^2} \right]^{-1} \quad (16)$$

with $C = \sqrt{\gamma_t} Q_0 / (2\pi F_0)$. Then for fixed self-propelled force F_0 , one can get higher transport efficiency with increasing input energy per-cycle Q_0 , and correspondingly the swimmer works with a torque Ω determined by the condition $Q_{cyc}(F_0, \Omega) = Q_0$. These serve as a reasonable design strategy for the swimmer, although how to transfer the input Q_0 to torque Ω may require specific technic.

As mentioned above, the lower bound for Q_{cyc} can be decreased with increasing k . Therefore, for given Q_0 , Q_0 / Q_{cyc}^{opt} will increase with k , i.e., the energy supply becomes more abundant with increasing k . Intuitively, the transport efficiency would become larger if all Q_0 is transferred to the torque. Unfortunately, it is not possible to get an analytical expression for $\chi_{\theta, \max}$ for $k \neq 0$. By numerical simulation, however, we indeed find that the maximum transport efficiency can be further improved by increasing k under the condition $Q_{cyc} \leq Q_0$, as illustrated below.

VIII. NUMERICAL SIMULATIONS

To test our previous theoretical predictions, we numerically solve the Langevin equation 1 and 2 with a time step 10^{-3} . The dissipation rate Σ is numerically

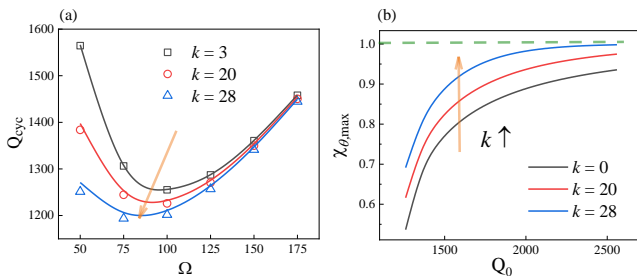


FIG. 3. (a) Cyclic cost Q_{cyc} as a function of the torque Ω for different values of the potential strength k . The optimal torque Ω_{opt} to minimize Q_{cyc} moves to the left, and the cyclic energy cost can be further reduced by increasing the potential strength. Lines: theory. Symbols: simulations. (b) The maximal transport efficiency $\chi_{\theta,max}$ as a function of the limited energy supply Q_0 for different values of the potential strength k . The maximal transport efficiency can also be enhanced by increasing the potential strength. The data is obtained from maximizing the analytical results for transport efficiency $\chi_{\theta} = F_0^2 / (F_0^2 + \gamma_t \Omega^2 + \gamma_t^{-1} k^2)$ under the constraint $Q_{cyc} \leq Q_0$. $F_0 = 100$.

calculated by using $\Sigma = T \langle \dot{s}_m \rangle$, i.e., Eq.(5), and D_{θ} is computed according to the definition. The precision-dissipation trade-off relation, Eq.(14), has been shown in Fig.2. It can be observed that the normalized phase diffusion constant $D = D_{\theta}/T$ is inversely proportional to the dissipation rate $\Sigma - \Sigma_c$, and the data plotted in log-log scale are fitted very well by a line with slope -1, in good agreement with the theoretical results.

In Fig.3(a), we show how the cyclic energy cost Q_{cyc} changes with the internal torque Ω , and the optimal torque Ω_{opt} can be clearly identified. As discussed above, the cyclic energy cost can be further reduced by increasing the potential strength k . At last, for different values of the potential strength k , the maximal transport efficiency $\chi_{\theta,max}$ under limited energy resource Q_0 is shown in Fig.3(b) for fixed $F_0 = 100$. Clearly, $\chi_{\theta,max}$ increases with Q_0 and approaching the upper bound 1 for very large energy input Q_0 , and introducing external potential will further improve the maximal transport efficiency, in consistent with our previous predictions.

IX. CONCLUSION

In summary, we have studied the stochastic thermodynamics for the Brownian circle swimmer in a 2D plane. We theoretically obtain an expression of the cost rate Σ , and an optimal torque for minimal cyclic cost Q_{cyc}

has been found, which provides the lower bound for the thermodynamic cost to sustain a stable circular motion. Meanwhile, it has been revealed that extra energy supply could be applied to enhance the precision of the transport process by a derived trade-off relation. Using the general principles for dissipative processes, the TURs, we also analyze the transport efficiency of cargo transport, which offers quantitative insight into the performance of the swimmer. Furthermore, we predict design strategies under the condition when the cyclic energy resource is limited. Analysis shows that the maximum χ_{θ} gradually approaches the upper bound while increasing the cyclic supply, which can be further enhanced by introducing an external potential. By using our approach, it is possible to design the swimmer for other important conditions, which is left for further investigation in future work.

Recently, the collective effects in active systems have attracted much attention⁶⁹. According to our main result (Eq.15), the transport efficiency reads as $\chi_{\theta} = (v_{\theta}^{st})^2 / \dot{S}_{tot} D_{\theta} = F_0^2 / (F_0^2 + \gamma_t \Omega^2 + \gamma_t^{-1} k^2)$, where F_0 is the self-propelled force, Ω is the torque and k is the potential strength. The steric interactions may induce an effective larger k , which will result a decreased transport efficiency. On the other hand, collective interactions could make the swimmers synchronize, which suppress the phase diffusion (smaller phase diffusion constant D_{θ}) to enhance the transport efficiency^{70,71}. Besides, the macroscopic crowding as a result of the inter-particle interactions may also enhance the transport efficiency by suppressing the torque Ω ⁷². In our opinion, the generalization to collective active systems is not straightforward, which deserves further study. Since it has been shown that various experimental setups are feasible to realize the swimmer model²⁴, we believe that the predicted principles and strategies presented here are testable, and can offer guidelines for experiments.

ACKNOWLEDGMENTS

This work is supported by MOST(2018YFA0208702), NSFC (32090044, 21973085, 21833007, 21790350, 21521001).

DATA AVAILABILITY

The data that support the findings of this study are available within the article and its supplementary material.

SUPPLEMENTARY INFORMATION

Appendix A: Cost rate for the circle swimmer

We now calculate the cost rate in steady state. Following Eq.(6) of the main text, the energy dissipation rate $\Sigma = \dot{Q} = T\dot{S}_{tot}$ reads

$$\Sigma = \int d\mathbf{r}d\varphi (\gamma_t v_r^2 + \gamma_r v_\varphi^2) P_{ss}(\mathbf{r}, \varphi) = \Sigma_r + \Sigma_c.$$

Here, $\Sigma_r = \gamma_t \langle v_r^2 \rangle$ and $\Sigma_c = \gamma_r \langle v_\varphi^2 \rangle$ denote the cost rate associated with the rotational motion along the circular orbit and the self chiral motion. Due to the time scale separation between the radial motion and the angular/chiral motion, Σ_r can be calculated by approximating $P_{ss}(\mathbf{r}, \varphi) \simeq P_{ss}(\mathbf{r})P_{ss}(\varphi)$ and $\langle r^2 \rangle \simeq r_m^2$ ^{58,59}

$$\Sigma_r \simeq \gamma_t \int \int r^2 \omega^2 P_{ss}(r, \theta) \cdot r dr d\theta \simeq \gamma_t \omega^2 \langle r^2 \rangle \simeq \gamma_t \omega^2 r_m^2. \quad (\text{A1})$$

The explicit expression for Σ_r reads

$$\Sigma_r = \frac{F_0^2 \Omega^2}{\gamma_t \Omega^2 + \gamma_t^{-1} k^2}. \quad (\text{A2})$$

As $\Sigma_c \simeq \Omega^2$, the cost rate can be derived as the form of Eq.(10) in the main text.

Appendix B: Design strategies for limited energy resource

By writing $\rho = \sqrt{\gamma_t} \Omega / F_0$, the design strategies emerges from maximizing the transport efficiency $\chi_\theta = 1 / (1 + \rho^2)$ under the condition that $2 \leq \rho + \rho^{-1} \leq \sqrt{\gamma_t} Q_0 / (2\pi F_0) = C$, where C is the dissipation normalized by self-propelled force. By solving for the range of the ratio that satisfies the condition, $\frac{2}{C + \sqrt{C^2 - 4}} \leq \rho \leq \frac{C + \sqrt{C^2 - 4}}{2}$, we can obtain the highest transport efficiency

$$\chi_{\theta, \max} = \frac{1}{1 + \rho_{\min}^2} \quad (\text{B1})$$

with $\rho_{\min} = \frac{2}{C + \sqrt{C^2 - 4}}$. We find that the available supply need to be fully utilized to enhance the transport efficiency.

Further, we start to analyze the effect of the external potential. Similarly, the question emerges from how to maximize the transport efficiency $\frac{1}{1 + F_0^{-2}(\Omega^2 + k^2)}$ under the condition $\frac{F_0^2 \Omega}{\Omega^2 + k^2} + \Omega \leq \frac{Q_0}{2\pi}$. By simply rewriting, the transport efficiency reads

$$\chi_\theta = \left(1 + \frac{\Omega}{\frac{Q_0}{2\pi} - \Omega} \right)^{-1}, \quad (\text{B2})$$

i.e., the smaller the torque allowed to be selected, the transport efficiency will be higher. For simplicity, we assume the potential strength k is relatively small. Approximating by Taylor expansion, the condition reads $\frac{F_0^2}{\Omega} + \Omega \lesssim \frac{Q_0}{2\pi} + \frac{F_0^2 k^2}{\Omega^3}$, which implies that the allowed torque is smaller by increasing the potential strength, i.e., the maximal transport efficiency can be further enhanced.

Appendix C: Numerical details

The starting point for the numerical simulations are Eqs.1 and 2, which are discretized according to the Euler's method as

$$\gamma_t [\mathbf{r}(t + \Delta t) - \mathbf{r}(t)] = \mathbf{F}_k(\mathbf{r}(t)) \Delta t + F_0 \mathbf{e}(t) \Delta t + \sqrt{2\gamma_t T \Delta t} \mathbf{I} \mathbf{N}_\xi, \quad (\text{C1})$$

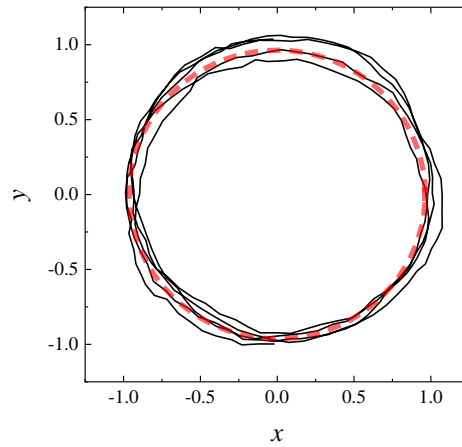


FIG. S1. Typical simulated trajectory in the xy plane (black lines) from Eqs.1 and 2. Here, $F_0 = 100$, $\Omega = 100$, $k = 28$, $T = 0.1$ and $\gamma_t = 1$. The red dashed circle represents the stationary circular orbit with the radius $r_m = F_0/\sqrt{\gamma_t^2\Omega^2 + k^2}$.

$$\varphi(t + \Delta t) - \varphi(t) = \Omega\Delta t + \sqrt{2T\Delta t}N_\zeta \quad (\text{C2})$$

with $\mathbf{r} = (x, y)$ and $\mathbf{e} = (\cos \varphi, \sin \varphi)$. \mathbf{N}_ξ and N_ζ are independent and normally distributed random variables with zero mean and unit variance. The discretized time step $\Delta t = 10^{-3}$, the translational friction coefficient $\gamma_t = 1$, and the statistical data are obtained from averaging over 10^4 trajectories. Typical trajectory in the xy plane of the numerical results is plotted in Fig.S1 (also can be seen Movie S1).

The most important quantities to be calculated are the thermodynamic cost rate Σ and transport efficiency χ_θ . Here, we use $\Sigma = T\langle \dot{s}_m \rangle = T\dot{S}_{tot}$ to calculate the thermodynamic cost rate. As discussed in the main text, $Tds_m = (\mathbf{F} + F_0\mathbf{e}) \cdot d\mathbf{r} + \Omega d\varphi$. Since $d\mathbf{r}$ and $d\varphi$ can be obtained from the dynamics generating from Eqs.1 and 2, ds_m or \dot{s}_m can be calculated numerically. By averaging over trajectories in steady states, the thermodynamic rate Σ can then be obtained. Moreover, the transport efficiency $\chi_\theta = (v_\theta^{st})^2/\dot{S}_{tot}D_\theta$, are obtained from the numerical data of \dot{S}_{tot} , v_θ^{st} and D_θ . As shown above, \dot{S}_{tot} can be obtained from simulations. As $\mathbf{r} = re^{i\theta}$, r and θ can be got from the generating dynamics, i.e., $v_\theta^{st} = \lim_{t \rightarrow \infty} \langle \dot{\theta} \rangle / t$ and $D_\theta = \lim_{t \rightarrow \infty} (\langle \theta^2 \rangle - \langle \theta \rangle^2) / 2t$ can also be calculated from the steady state trajectories. Therefore, the transport efficiency can be obtained from the simulated data.

- ¹A. M. Menzel, Physics reports **554**, 1 (2015).
- ²A. P. Solon, M. Cates, and J. Tailleur, The European Physical Journal Special Topics **224**, 1231 (2015).
- ³C. Weber, P. K. Radtke, L. Schimansky-Geier, and P. H"anggi, Physical Review E **84**, 011132 (2011).
- ⁴D. Debnath, P. K. Ghosh, Y. Li, F. Marchesoni, and B. Li, Soft Matter **12**, 2017 (2016).
- ⁵B. Ten Hagen, R. Wittkowski, D. Takagi, F. K"ummel, C. Bechinger, and H. L"owen, Journal of Physics: Condensed Matter **27**, 194110 (2015).
- ⁶S. Ramaswamy, Annu. Rev. Condens. Matter Phys. **1**, 323 (2010).
- ⁷P. Romanczuk, M. B"ar, W. Ebeling, B. Lindner, and L. Schimansky-Geier, The European Physical Journal Special Topics **202**, 1 (2012).
- ⁸T. Vicsek and A. Zafeiris, Physics reports **517**, 71 (2012).
- ⁹M. C. Marchetti, J.-F. Joanny, S. Ramaswamy, T. B. Liverpool, J. Prost, M. Rao, and R. A. Simha, Reviews of Modern Physics **85**, 1143 (2013).
- ¹⁰J. Elgeti, R. G. Winkler, and G. Gompper, Reports on progress in physics **78**, 056601 (2015).
- ¹¹C. Bechinger, R. Di Leonardo, H. L"owen, C. Reichhardt, G. Volpe, and G. Volpe, Reviews of Modern Physics **88**, 045006 (2016).
- ¹²O. Raz and A. Leshansky, Physical Review E **77**, 055305 (2008).
- ¹³E. Gutman and Y. Or, Physical Review E **93**, 063105 (2016).
- ¹⁴X. Ma, K. Hahn, and S. Sanchez, Journal of the American Chemical Society **137**, 4976 (2015).
- ¹⁵A. F. Demir"ors, M. T. Akan, E. Poloni, and A. R. Studart, Soft Matter **14**, 4741 (2018).
- ¹⁶T. Debnath and P. K. Ghosh, Physical Chemistry Chemical Physics **20**, 25069 (2018).
- ¹⁷S. van Teeffelen, U. Zimmermann, and H. L"owen, Soft Matter **5**, 4510 (2009).
- ¹⁸C. Reichhardt and C. O. Reichhardt, Physical Review E **88**, 042306 (2013).
- ¹⁹F. K"ummel, B. ten Hagen, R. Wittkowski, I. Buttinoni, R. Eichhorn, G. Volpe, H. L"owen, and C. Bechinger, Physical review letters **110**, 198302 (2013).
- ²⁰Y. Yang, F. Qiu, and G. Gompper, Physical Review E **89**, 012720 (2014).
- ²¹X. Ao, P. K. Ghosh, Y. Li, G. Schmid, P. H"anggi, and F. Marchesoni, EPL (Europhysics Letters) **109**, 10003 (2015).
- ²²W. Schirmacher, B. Fuchs, F. H"offling, and T. Franosch, Physical review letters **115**, 240602 (2015).
- ²³A. Geiseler, P. H"anggi, F. Marchesoni, C. Mulhern, and S. Savel'ev, Physical Review E **94**, 012613 (2016).
- ²⁴S. Jahanshahi, H. L"owen, and B. Ten Hagen, Physical Review E **95**, 022606 (2017).
- ²⁵H. L"owen, Physical Review E **99**, 062608 (2019).

- ²⁶J. Su, H.-J. Jiang, and Z.-H. Hou, *The Journal of Physical Chemistry C* **123**, 17624 (2019).
- ²⁷J. Su, H. Jiang, and Z. Hou, *Soft Matter* **15**, 6830 (2019).
- ²⁸I. S. Khalil, V. Magdanz, S. Sanchez, O. G. Schmidt, and S. Misra, *Journal of Micro-Bio Robotics* **9**, 79 (2014).
- ²⁹V. Magdanz, S. Sanchez, and O. G. Schmidt, *Advanced Materials* **25**, 6581 (2013).
- ³⁰V. Magdanz, M. Guix, F. Hebenstreit, and O. G. Schmidt, *Advanced materials* **28**, 4084 (2016).
- ³¹S. Fournier-Bidoz, A. C. Arsenault, I. Manners, and G. A. Ozin, *Chemical Communications* pp. 441–443 (2005).
- ³²N. A. Marine, P. M. Wheat, J. Ault, and J. D. Posner, *Physical Review E* **87**, 052305 (2013).
- ³³D. Takagi, A. B. Braunschweig, J. Zhang, and M. J. Shelley, *Physical review letters* **110**, 038301 (2013).
- ³⁴J. Buzhardt and P. Tallapragada, *ASME Letters in Dynamic Systems and Control* **1** (2021).
- ³⁵B. Liebchen and H. L’owen, *EPL (Europhysics Letters)* **127**, 34003 (2019).
- ³⁶S. van Teeffelen and H. L’owen, *Physical Review E* **78**, 020101 (2008).
- ³⁷P. Muratore-Ginanneschi and K. Schwiager, *Physical Review E* **90**, 060102 (2014).
- ⁵³T. Nemoto, E. Fodor, M. E. Cates, R. L. Jack, and J. Tailleur, *Physical Review E* **99**, 022605 (2019).
- ⁵²P. Pietzonka, E. Fodor, C. Lohrmann, M. E. Cates, and U. Seifert, *Physical Review X* **9**, 041032 (2019).
- ⁴⁰U. Seifert, *Reports on progress in physics* **75**, 126001 (2012).
- ⁴¹U. Seifert, *The European Physical Journal B* **64**, 423 (2008).
- ⁴²U. Seifert, *Annual Review of Condensed Matter Physics* **10**, 171 (2019).
- ⁴³C. Jarzynski, *Annu. Rev. Condens. Matter Phys.* **2**, 329 (2011).
- ⁴⁴A. C. Barato and U. Seifert, *Physical review letters* **114**, 158101 (2015).
- ⁴⁵W. Hwang and C. Hyeon, *The journal of physical chemistry letters* **9**, 513 (2018).
- ⁴⁶É. Fodor, C. Nardini, M. E. Cates, J. Tailleur, P. Visco, and F. van Wijland, *Physical review letters* **117**, 038103 (2016).
- ⁴⁷D. J. Pearce and L. Giomi, *Physical Review E* **94**, 022612 (2016).
- ⁴⁸N. Kyriakopoulos, F. Ginelli, and J. Toner, *New Journal of Physics* **18**, 073039 (2016).
- ⁴⁹D. Mandal, K. Klymko, and M. R. DeWeese, *Physical review letters* **119**, 258001 (2017).
- ⁵⁰P. Pietzonka and U. Seifert, *Journal of Physics A: Mathematical and Theoretical* **51**, 01LT01 (2017).
- ⁵¹S. Shankar and M. C. Marchetti, *Physical Review E* **98**, 020604 (2018).
- ⁵²P. Pietzonka, É. Fodor, C. Lohrmann, M. E. Cates, and U. Seifert, *Physical Review X* **9**, 041032 (2019).
- ⁵³T. Nemoto, É. Fodor, M. E. Cates, R. L. Jack, and J. Tailleur, *Physical Review E* **99**, 022605 (2019).
- ⁵⁴L. Dabelow, S. Bo, and R. Eichhorn, *Physical Review X* **9**, 021009 (2019).
- ⁵⁵E.W. Burkholder and J.F. Brady, *The Journal of chemical physics* **150**, 184901 (2019).
- ⁵⁶L.L. Bonilla, *Physical Review E* **100**, 022601 (2019).
- ⁵⁷G. Szamel, *Physical Review E* **100**, 050603 (2019).
- ⁵⁸Z. Cao, H. Jiang, and Z. Hou, *Physical Review Research* **2**, 043331 (2020).
- ⁵⁹Y. Cao, H. Wang, Q. Ouyang, and Y. Tu, *Nature Physics* **11**, 772 (2015).
- ⁶⁰J. M. Horowitz and T. R. Gingrich, *Nature Physics* pp. 1–6 (2019).
- ⁶¹T. R. Gingrich, J. M. Horowitz, N. Perunov, and J. L. England, *Physical review letters* **116**, 120601 (2016).
- ⁶²P. Pietzonka, A. C. Barato, and U. Seifert, *Physical Review E* **93**, 052145 (2016).
- ⁶³S. Pigolotti, I. Neri, E. Roldán, and F. J’ulicher, *Physical review letters* **119**, 140604 (2017).
- ⁶⁴K. Proesmans and C. Van den Broeck, *EPL (Europhysics Letters)* **119**, 20001 (2017).
- ⁶⁵A. Dechant and S.-i. Sasa, *Physical Review E* **97**, 062101 (2018).
- ⁶⁶T. Van Vu and Y. Hasegawa, *Physical Review E* **100**, 032130 (2019).
- ⁶⁷Y. Hasegawa and T. Van Vu, *Physical Review Letters* **123**, 110602 (2019).
- ⁶⁸A. Dechant and S.-i. Sasa, *Journal of Statistical Mechanics: Theory and Experiment* **2018**, 063209 (2018).
- ⁶⁹T. F. Farage, P. Krinninger, and J. M. Brader, *Physical Review E* **91**, 042310 (2015).
- ⁷⁰D. Zhang, Y. Cao, Q. Ouyang, and Y. Tu, *Nature Physics* (2020).
- ⁷¹S. Lee, C. Hyeon, and J. Jo, *Physical Review E* **98**, 032119 (2018).
- ⁷²I. M. Sokolov, *Soft Matter* **8**, 9043 (2012).